Mass Transfer Dynamics of the Evaporation Step in Membrane Formation by Phase Inversion

Ji Hua Hao, Shichang Wang

School of Chemical Engineering, Tianjin University, Tianjin 300072, People's Republic of China

Received 12 September 2001; accepted 14 January 2002

ABSTRACT: A ternary diffusion model has been developed for the evaporation step of the phase inversion process. The model is applied to the analysis of mass transfer dynamics of the evaporation step for the methanol–acetone–cellulose acetate (CA) ternary casting system. The combined analysis of quantitatively computational results from the ternary evaporation model and qualitative dynamic results during the quench process has shown that the evaporation step is essentially necessary to prepare the defect-free, ultrathin skinned asymmetric CA membrane for the separation of CO_2/CH_4. The skin layer of high CA concentration obtained by evaporation has an ability to suppress liquid–liquid phase separation. And the skin layer with high tensile strength can resist the interfacial tension caused by spinodal decomposition from the substructure. Although the CA concentration in the skin layer increases considerably because of the evaporation step and the following delay time during the quench process, the substructure can still induce the spinodal decomposition because the strong coagulant, methanol, can diffuse rapidly across the ultrathin skin layer. Hence the defect-free, ultrathin-skinned asymmetric membrane for gas separation can be prepared from methanol–acetone–CA casting system by evaporation step and the wet phase inversion. © 2002 Wiley Periodicals, Inc. J Appl Polym Sci 86: 1564–1571, 2002

Key words: diffusion; evaporation model; integrally skinned; theory

INTRODUCTION

Integrally skinned asymmetric gas separation membranes were prepared by dry, wet, and dry/wet phase inversion processes.[1–5] Pinnau et al. fabricated essentially defect-free integrally skinned asymmetric polysulfone membranes by dry/wet phase inversion process using forced-convective evaporation.[2, 3] Hao et al. prepared integrally skinned asymmetric cellulose acetate membranes by the wet phase inversion.[4, 5] The evaporation step was thus determined to be a key to the formation of integrally defect-free skin by the inversion process. To analyze the formation mechanism on the integrally skinned defect-free asymmetric membrane, a diffusion model has to be developed for accurately describing the diffusion phenomena during evaporation, especially concentration profiles in the polymer film during evaporation.

However, the general assumptions for all evaporation models are those of polymer–solvent binary diffusion. From the earliest evaporation models presented by Anderson and Ullman,[6] Ataka and Sasaki,[7] Castellaru and Ottani,[8, 9] and Krantz[10] to the mass transfer dynamics model of the evaporation step presented by Tsay and McHugh,[11] and Wang,[12] the diffusion models for the evaporation step have been improved gradually on the basis of their rigorous, reasonable form and ability to predict the actual composition in the polymer film during the evaporation. But most of the actual cast systems are involved in the ternary components or more. The binary diffusion models developed previously for the evaporation step have been unable to meet with the actual requirement. There is a clear and urgent need for the ternary mass transfer dynamics of the evaporation step in membrane formation by phase inversion process that incorporates the effect of the moving air–film interface, concentration dependence of the mutual diffusivity, and time-dependent mass transfer coefficient.

In the following sections, ternary diffusion models for the evaporation step are set up on the basis of the existing binary models and Tsay's ternary diffusion model to describe the mass transfer processes associated with the quench bath period of the phase inversion process for membrane formation.[11, 13, 14] We calculated the composition change during the evaporation for a specific membrane-forming system, methanol–acetone–cellulose acetate (CA). In addition, the role of evaporation was analyzed for the integrally skinned asymmetric CA membranes made by the wet phase inversion for removal of CO_2 from natural gas.[4, 5]

Correspondence to: J.H. Hao (haojh2001@yahoo.com).

Journal of Applied Polymer Science, Vol. 86, 1564–1571 (2002)

DEVELOPMENT OF EVAPORATION MODEL

The geometry of evaporation model is shown in Figure 1. Basic assumptions are: (1) one dimensional, iso-

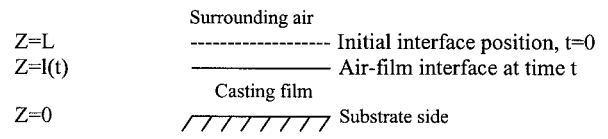

Figure 1 Schematic of coordinates defining evaporation geometry. The initial cast film interface is at L, and $l(t)$ represents an arbitrary location at time t of the same.

thermal, Fickian diffusion; (2) polymer–solvent–nonsolvent ternary system; (3) no volume change on mixing; (4) ideal gas behavior on air side; (5) gas–liquid equilibrium at the air–film interface.

Starting from first principles,[15] the following three continuity equations hold for one-dimensional transfer:

$$\frac{\partial \rho}{\partial t} = -\frac{\partial}{\partial z}(n_1 + n_2 + n_3) \tag{1}$$

$$\frac{\partial \rho_1}{\partial t} = -\frac{\partial n_1}{\partial z} \tag{2}$$

$$\frac{\partial \rho_2}{\partial t} = -\frac{\partial n_2}{\partial z} \tag{3}$$

where ρ_i and n_i are, respectively, the mass concentration and mass flux of component i with respect to fixed coordinates. The subscripts refer to nonsolvent (1), solvent (2), and polymer (3). Consistent with the use of modified Flory–Huggins theory for solution thermodynamics, we assume constant partial specific volume. As a consequence, the bulk flow terms associated with the volume-average velocity can be shown to be identically zero,[16] and therefore n_i becomes identical to the mass flux of component i with respect to the volume-average velocity. In this way, volume fraction of component ϕ_i can replace ρ_i. To facilitate numerical calculations, the following coordinate transformation is used to immobilize the interface position:

$$\eta = \frac{z}{l} \tag{4}$$

The final set of diffusion equations in the film side can be written in dimensionless form as follows:[13, 14]

$$\frac{\partial \phi_1}{\partial t} = \frac{\eta}{l}\frac{\mathrm{d}l}{\mathrm{d}t}\frac{\partial \phi_1}{\partial \eta} + \frac{1}{l^2}\frac{\partial}{\partial \eta}\left(\frac{D_{11}}{D_0}\frac{\partial \phi_1}{\partial \eta} + \frac{\hat{V}_1}{\hat{V}_2}\frac{D_{12}}{D_0}\frac{\partial \phi_2}{\partial \eta}\right) \tag{5}$$

$$\frac{\partial \phi_2}{\partial t} = \frac{\eta}{l}\frac{\mathrm{d}l}{\mathrm{d}t}\frac{\partial \phi_2}{\partial \eta} + \frac{1}{l^2}\frac{\partial}{\partial \eta}\left(\frac{\hat{V}_2}{\hat{V}_1}\frac{D_{21}}{D_0}\frac{\partial \phi_1}{\partial \eta} + \frac{D_{22}}{D_0}\frac{\partial \phi_2}{\partial \eta}\right) \tag{6}$$

Initial conditions:

$$\phi_1(\eta, 0) = \phi_{10} \quad 0 \le \eta \le 1 \tag{7}$$

$$\phi_2(\eta, 0) = \phi_{20} \quad 0 \le \eta \le 1 \tag{8}$$

Boundary conditions:

The boundary conditions between the membrane and the support:

$$\frac{\partial \phi_1}{\partial \eta} = 0 \quad \eta = 0 \tag{9}$$

$$\frac{\partial \phi_2}{\partial \eta} = 0 \quad \eta = 0 \tag{10}$$

The boundary conditions of the film-air interface can get by the mass transfer equilibrium:

$$\frac{\mathrm{d}}{\mathrm{d}t}\int_0^{l_{(t)}} \rho_1 \mathrm{d}z = -k_1(\rho_{1gt} - \rho_{1g\infty}) \quad z = l_{(t)} \tag{11}$$

$$\frac{\mathrm{d}}{\mathrm{d}t}\int_0^{l_{(t)}} \rho_2 \mathrm{d}z = -k_2(\rho_{2gt} - \rho_{2g\infty}) \quad z = l_{(t)} \tag{12}$$

where ρ_i, t, and z represent the mass density of component i, time, and position, respectively; k is the gas side mass-transfer coefficient; and the subscripts 0, g, t, and ∞ refer respectively to the initial value, gas phase side, air–film interface, and position away from the interface. Conservation of polymer mass gives the following equation for the moving interface:

$$\int_0^{l_{(t)}} \rho_3 \mathrm{d}z = \int_0^{L} \rho_{30} \mathrm{d}z \tag{13}$$

Because ideal gas and equilibrium are assumed, the compositions of solvent and nonsolvent at the gas side of the interface can be written in terms of the activities of solvent (a_1) and nonsolvent (a_2) on the polymer film side as:[17]

$$\rho_{1gt} = a_1 P_1^{\mathrm{sat}} / \hat{V}_{1\mathrm{g}} P \tag{14}$$

$$\rho_{2gt} = a_2 P_2^{\mathrm{sat}} / \hat{V}_{2\mathrm{g}} P \tag{15}$$

where P is the total pressure, P_i^{sat} is the pure solvent or nonsolvent vapor pressure, and V_{ig} is the partial specific volume of the solvent and nonsolvent in the gas phase. The activities are evaluated from chemical potential of components i:[17]

$$a_i = \exp(\Delta\mu_i / RT) \tag{16}$$

where $\Delta\mu_i$ can be obtained from Flory–Huggins theory:[18]

$$\Delta\mu_1/RT = \ln\phi_1 + 1 - \phi_1 - \frac{\nu_1}{\nu_2}\phi_2 - \frac{\nu_1}{\nu_3}\phi_3 + (g_{12}\phi_2 + g_{13}\phi_3)(\phi_2 + \phi_3) - g_{23}\frac{\nu_1}{\nu_2}\phi_2\phi_3 - u_1u_2\phi_2\left(\frac{dg_{12}}{du_2}\right) - \phi_1Y_3^2\left(\frac{dg_{13}}{dY_3}\right) \quad (17)$$

$$\Delta\mu_2/RT = \ln\phi_2 + 1 - \phi_2 - \frac{\nu_2}{\nu_1}\phi_1 - \frac{\nu_2}{\nu_3}\phi_3 + \left(g_{12}\frac{\nu_2}{\nu_1}\phi_1 + g_{23}\phi_3\right)(\phi_1 + \phi_3) - g_{13}\frac{\nu_2}{\nu_1}\phi_1\phi_3 + u_1u_2\frac{\nu_2}{\nu_1}\phi_1\left(\frac{dg_{12}}{du_2}\right) - \phi_2W_3^2\left(\frac{dg_{23}}{dW_3}\right) \quad (18)$$

where ϕ_i is the volume fraction of component i; R and T have their usual significance of gas constant and temperature, respectively; g_{12} is the solvent–nonsolvent interaction parameter and it is assumed to be a function of u_2; g_{13} is the nonsolvent–polymer interaction parameter and it is assumed to be a function of Y_3; g_{23} is the solvent–polymer interaction parameter and it is assumed to be a function of W_2. The quantities u_1 and u_2 are given by $u_1 = \phi_1/(\phi_1 + \phi_2)$, and $u_2 = \phi_2/(\phi_1 + \phi_2)$. The quantities Y_1 and Y_3 are given by $Y_1 = \phi_3/(\phi_1 + \phi_3)$, and $Y_3 = \phi_3/(\phi_1 + \phi_3)$. The quantities W_2 and W_3 are given by $W_2 = \phi_2/(\phi_2 + \phi_3)$, $W_3 = \phi_3/(\phi_2 + \phi_3)$.

Because evaporation is usually carried out under free convection conditions, the following expression for the mass transfer coefficient k is appropriate:[19]

$$\frac{k_iL_cy_{iair,lm}}{D_{ig}} = 0.27(Gr_iSc_i)^{0.25}\ (10^5 \le Gr_iSc_i \le 10^{10}) \quad (19)$$

where $y_{iair,lm}$ is the log mean mole fraction difference of the air, and L_c and D_g are, respectively, a characteristic length of the film surface and the mutual diffusion coefficient of the air–solvent gas phase. The Grashof and Schmidt numbers have their standard definitions:

$$Gr_i = \frac{L_c^3\rho_g^2g|\zeta_i(y_{igt} - y_{ig\infty})|}{\mu_g^2} \quad (20)$$

$$Sc_i = \frac{\mu_g}{\rho_gD_{ig}} \quad (21)$$

where ρ_g, g, and μ_g represent the total mass density of gas phase, the gravitational constant, and viscosity of gas mixture, respectively. The coefficient ζ represents the effect of the concentration profile on the gas density and is given by:

$$\zeta_i = -\frac{1}{\rho_g}\left(\frac{\partial\rho_g}{\partial y_i}\right)_{P,T} \quad (22)$$

After substitution of eqs. 20–22 into eq. 19, the equation for the mass transfer coefficient k can become

$$k_1 = \frac{0.27}{y_{1air,lm}}\left(\frac{PgD_{1g}^3|(M_{air} - M_1)(y_{1gt} - y_{1g\infty})|}{RTL_c\mu_g}\right)^{0.25} \quad (23)$$

$$k_2 = \frac{0.27}{y_{2air,lm}}\left(\frac{PgD_{2g}^3|(M_{air} - M_2)(y_{2gt} - y_{2g\infty})|}{RTL_c\mu_g}\right)^{0.25} \quad (24)$$

Application of the similar coordinate transformation $\eta = z/l$ for eqs. 11–13 along with substitution of the volume fraction as the independent variable for constant partial specific volume, leads to the other two boundary conditions for eqs. 5 and 6:

$$\frac{d}{dt}\left(l\int_0^1\phi_1d\eta\right) = -\frac{k_1\hat{V}_1}{\hat{V}_{1g}}\left(\frac{P_1^{sat}}{P}a_1 - y_{1g\infty}\right) \quad \eta = 1 \quad (25)$$

$$\frac{d}{dt}\left(l\int_0^1\phi_2d\eta\right) = -\frac{k_2\hat{V}_2}{\hat{V}_{2g}}\left(\frac{P_2^{sat}}{P}a_2 - y_{2g\infty}\right) \quad \eta = 1 \quad (26)$$

where

$$l = L\frac{\int_0^1\phi_{30}d\eta}{\int_0^1\phi_3d\eta} \quad (27)$$

The numerical calculations are carried out using the algorithm published in references 5 and 14.

DETERMINATION OF MODEL PARAMETERS

Ternary diffusion coefficients

Consistent with the assumption of constant molar volume, we will use the formulation for the diffusion coefficients derived by Vrentas et al.[20] Rewriting their results in terms of volume fraction gives the following:

$$D_{11} = -\frac{\hat{V}_1}{N_A^2E}\left(E_{22}\frac{\partial\mu_1}{\partial\phi_1} - E_{12}\frac{\partial\mu_2}{\partial\phi_1}\right) \quad (28)$$

$$D_{12} = -\frac{\hat{V}_2}{N_A^2E}\left(E_{22}\frac{\partial\mu_1}{\partial\phi_2} - E_{12}\frac{\partial\mu_2}{\partial\phi_2}\right) \quad (29)$$

$$D_{21} = -\frac{\hat{V}_1}{N_A^2E}\left(E_{11}\frac{\partial\mu_2}{\partial\phi_1} - E_{21}\frac{\partial\mu_1}{\partial\phi_1}\right) \quad (30)$$

$$D_{22} = -\frac{\hat{V}_2}{N_A^2 E}\left(E_{11}\frac{\partial \mu_2}{\partial \phi_2} - E_{21}\frac{\partial \mu_1}{\partial \phi_2}\right) \tag{31}$$

where N_A is Avogadro's number and D_{ij} is the phenomenological ternary diffusion coefficient at casting film side.

$$E_{11} = \frac{\hat{V}_1\phi_2\zeta_{12}}{\nu_2\phi_3} - \frac{RT\hat{V}_1(1-\phi_2)}{N_A^2 D_{T1}\phi_1\phi_3} \tag{32}$$

$$E_{12} = \frac{(1-\phi_1)\zeta_{12}}{M_2\phi_3} - \frac{RT\hat{V}_2}{N_A^2 D_{T1}\phi_3} \tag{33}$$

$$E_{21} = \frac{(1-\phi_2)\zeta_{12}}{M_1\phi_3} - \frac{RT\hat{V}_1}{N_A^2 D_{T2}\phi_3} \tag{34}$$

$$E_{22} = \frac{\hat{V}_2\phi_1\zeta_{12}}{\nu_1\phi_3} - \frac{RT\hat{V}_2(1-\phi_1)}{N_A^2 D_{T2}\phi_2\phi_3} \tag{35}$$

$$E = -\frac{\zeta_{12}^2}{M_1M_2\phi_3} + \frac{R^2T^2\hat{V}_1\hat{V}_2}{N_A^4 D_{T1}D_{T2}\phi_1\phi_2\phi_3} \tag{36}$$

$$D_{T1} = \frac{RT}{N_A^2\left(\frac{\phi_2\zeta_{12}}{\nu_2} + \frac{\phi_3\zeta_{13}}{\nu_3}\right)} \tag{37}$$

$$D_{T2} = \frac{RT}{N_A^2\left(\frac{\phi_1\zeta_{12}}{\nu_1} + \frac{\phi_3\zeta_{23}}{\nu_3}\right)} \tag{38}$$

where, M_i and v_i are the molecular weight and pure molar volume of component i, respectively, and ζ_{ij} represents the friction coefficient between components i and j. Expression for the chemical potentials and their derivatives are given from eqs. 17 and 18:

$$\frac{\partial(\Delta\mu_1/RT)}{\partial\phi_1} = \frac{1}{\phi_1} - 1 + \frac{\nu_1}{\nu_3} + \phi_2\left(\frac{\nu_1}{\nu_2}g_{23} - g_{12}\right) - g_{13}(\phi_2 + 2\phi_3) + u_2^2(u_1 - u_2 - \phi_2 - \phi_3)\frac{dg_{12}}{du_2} + Y_3(2Y_1 - Y_3 - \phi_2 - \phi_3)\frac{dg_{13}}{dY_3} + \frac{\nu_1}{\nu_2}\phi_2 W_2 W_3\frac{dg_{23}}{dW_3} + u_1u_2^3\left(\frac{d^2g_{12}}{du_2^2}\right) + Y_1Y_3^2\left(\frac{d^2g_{13}}{dY_3^2}\right) \tag{39}$$

$$\frac{\partial(\Delta\mu_1/RT)}{\partial\phi_2} = \frac{\nu_1}{\nu_3} - \frac{\nu_1}{\nu_2} + (\phi_2 + \phi_3)(g_{12} - g_{13}) + \frac{\nu_1}{\nu_2}g_{23}(\phi_2 - \phi_3) + u_1u_2(u_2 - u_1 - \phi_1)\frac{dg_{12}}{du_2} + Y_1Y_3(2Y_1 - \phi_2 - \phi_3)\frac{dg_{13}}{dY_3} + \frac{\nu_1}{\nu_2}\phi_2 W_3\frac{dg_{23}}{dW_3} - u_1^2u_2^2\left(\frac{d^2g_{12}}{du_2^2}\right) + Y_1Y_3^2\left(\frac{d^2g_{13}}{dY_3^2}\right) \tag{40}$$

$$\frac{\partial(\Delta\mu_2/RT)}{\partial\phi_1} = \frac{\nu_2}{\nu_3} - \frac{\nu_2}{\nu_1} + (\phi_1 + \phi_3)\left(\frac{\nu_2}{\nu_1}g_{12} - g_{23}\right) + (\phi_1 - \phi_3)\frac{\nu_2}{\nu_1}g_{13} + u_1u_2\frac{\nu_2}{\nu_1}(\phi_2 + u_2 - u_1)\frac{dg_{12}}{du_2} + W_2W_3(2W_2 - \phi_1 - \phi_3)\frac{dg_{23}}{dW_3} + \frac{\nu_2}{\nu_1}\phi_1 Y_3\frac{dg_{13}}{dY_3} - u_1^2u_2^2\frac{\nu_2}{\nu_1}\left(\frac{d^2g_{12}}{du_2^2}\right) + W_2^2W_3^2\left(\frac{d^2g_{23}}{dW_3^2}\right) \tag{41}$$

$$\frac{\partial(\Delta\mu_2/RT)}{\partial\phi_2} = \frac{1}{\phi_2} - 1 + \frac{\nu_2}{\nu_3} + \frac{\nu_2}{\nu_1}\phi_1(g_{13} - g_{12}) - g_{23}(\phi_1 + 2\phi_3) + u_1^2\frac{\nu_2}{\nu_1}(u_1 - u_2 + \phi_1 + \phi_3)\frac{dg_{12}}{du_2} + W_3(2W_2 - W_3 - \phi_1 - \phi_3)\frac{dg_{23}}{dW_3} + \frac{\nu_2}{\nu_1}\phi_3 Y_1\frac{dg_{13}}{dY_3} + u_1^3u_2\frac{\nu_2}{\nu_1}\left(\frac{d^2g_{12}}{du_2^2}\right) + W_2W_3^2\left(\frac{d^2g_{23}}{dW_3^2}\right) \tag{42}$$

The binary ζ_{12} and ζ_{23} are related to the mutual diffusion coefficient and sedimentation measurement and are given as:[13, 21, 22]

$$\zeta_{12} = \frac{\nu_2\phi_1}{N_A^2 D}\left(\frac{d\mu_1}{d\phi_1}\right) \tag{43}$$

$$\zeta_{23} = \frac{M_2\nu_3(1-\phi_3)(\rho\hat{V}_2 - 1)g}{N_A^2\phi_3 u_3} \tag{44}$$

where D, u_3, and g are the mutual diffusion coefficient, the polymer velocity with respect to fixed coordinates, and the centrifugal field, respectively.

Because reliable data for ζ_{13} by either diffusion or sedimentation measurements are generally not available, following Reuvers et al.,[13, 21] we will assume that the binary friction coefficients are proportional and therefore

$$\zeta_{13} = C\frac{\nu_1}{\nu_2}\zeta_{23} \tag{45}$$

where C is a constant. The value can best be estimated from diffusion data. To do so, we note that the self-diffusion coefficient of component 1 in a 1–3 binary system is defined as[20]

TABLE I
Model Parameters for the Cellulose Acetate-Acetone System

Parameter	Value
Molecular weight	$M_2 = 58.08$, $M_3 = 27000$ g/mol
Specific volume	$V_2 = 1.266$, $V_3 = 0.7634$
Initial film thickness	$L = 0.010$ cm
Characteristic diffusivity	$D_0 = 10^{-5}$ cm^2/s
Thermodynamic interaction parameter	$g_{23} = 0.535 + 0.11W_3$
Friction coefficient	$\zeta_{23} = (\nu_3 RT)/(1.66N_A^2) \times 10^{4+5.17W_3}$
Pure molar volume	$\nu_2 = 74.05$ $\nu_3 = 20000$ cm^3/g · mol

$$D_1 = \frac{RT}{N_A^2\left(\frac{\phi_1\zeta_{11}}{\nu_1} + \frac{\phi_3\zeta_{13}}{\nu_3}\right)} \tag{46}$$

Because ϕ_1 tends to zero, eq. 46 leads to

$$D_1 = \frac{\nu_3 RT}{N_A^2\zeta_{13}} = \frac{\nu_2\nu_3 RT}{N_A^2 C\nu_1\zeta_{23}} \tag{47}$$

Vrentas et al. have shown that D_1 is equal to the mutual diffusion coefficient, D, as $\phi_1 \to 0$.[20] Hence, the C value can be determined as soon as D and ζ_{23} are available. Some of the required model parameters for 25 °C and 1 atm are listed in Table I.

The relation between ζ_{13} and ζ_{23} is assumed in the form of eq. 45. In the limit of zero concentration of component 1 in the 1–3 binary system, application of eqs. 45 and 47 and Table I yields

$$D_{1\phi_1\to 0} = \frac{8.3 \times 10^{-8}}{C\nu_1}\ \text{cm}^2/\text{s} \tag{48}$$

$D_{\phi_1\to 0}$ and $D_{1\phi_1\to 0}$ for the binary system of acetone and methanol can be estimated from Wilke–Chung equation and experimental results from Laatikainen.[23, 24]

The value of D_g comes from reference 25 at 25 °C and 1 atm. Saturated vapor pressure comes from reference 26. Viscosity of pure material comes from reference 27. the μ_g values for polar gas mixtures are applicable.[28]

$$\mu_g = \sum_{i=1}^{n} \frac{y_i\mu_i^0}{\sum_{j=1}^{n} y_i\phi_{ij}} \tag{49}$$

$$\phi_{ij} = \left(\frac{\mu_i^0}{\mu_j^0}\right)^{0.5} S_{ij}A_{ij} \tag{50}$$

$$A_{ij} = m_{ij}M_{ij}^{-0.5} \times \left(1 + \frac{M_{ij} - M_{ij}^{0.45}}{2(1 + M_{ij}) + \frac{(1 + M_{ij}^{0.45})}{(1 + m_{ij})m_{ij}^{0.5}}}\right) \tag{51}$$

$$m_{ij} = \left(\frac{4}{(1 + M_{ij}^{-1})(1 + M_{ij})}\right)^{0.25} \tag{52}$$

$$M_{ij} = M_i/M_j \tag{53}$$

when $0.4 < M_i/M_j < 1.33$, and $A_{ij} = (M_i/M_j)^{-0.37}$, then

$$S_{ij} = \quad S_{ji} = \frac{1 + (T_i^*T_j^*)^{0.5} + \frac{\delta_i\delta_j}{4}}{\left(1 + T_i^* + \frac{\delta_i^2}{4}\right)^{0.5}\left(1 + T_j^* + \frac{\delta_j^2}{4}\right)^{0.5}} \tag{54}$$

$$T_i^* = \frac{T}{\varepsilon_i/k} \tag{55}$$

TABLE II
Model Parameters for the Cellulose Acetate–Acetone System

Parameter	Value
Molecular weight (g/gmol)	$M_{air} = 28.97$
Specific volume (cm^3/g)	$V_{1g} = 763.59$, $V_{2g} = 421.23$
Initial film thickness (cm)	$L = 0.010$, $L_c = 10$
Saturated vapor pressure (atm)	$P_2^{sat} = 0.3$, $P_1^{sat} = 0.172$
Diffusivity of air with acetone, methanol	$D_{2g} = 0.128$, $D_{1g} = 0.159$
Viscosity (cp.)	$\mu_2^0 = 0.077$, $\mu_{air}^0 = 0.018$, $\mu_1^0 = 0.0094$
Stockmayer parameter	$\delta_2 = 0.11$, $\delta_{air} = 0.0$, $\delta_1 = 0.5$
Lennard–Jones parameter	$\varepsilon_2/k = 560.2$, $\varepsilon_{air}/k = 78.6$, $\varepsilon_1/k = 481.0$

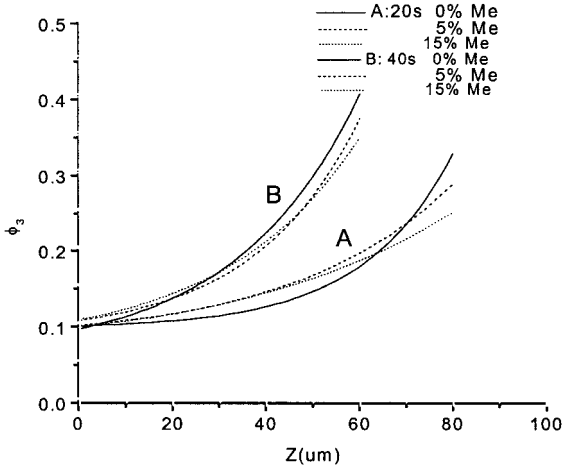

Figure 2 The effect of evaporation time on polymer concentration profile.

where δ_i and ε_i/k represent the Stockmayer parameter[29] and the Lennard–Jones parameter of component i,[30] respectively. The rest of the model parameters are listed in Table II.

ANALYSIS OF MASS TRANSFER DYNAMICS OF EVAPORATION STEP

Essentially defect-free integrally skinned asymmetric CA membranes were fabricated by the wet phase inversion process with an evaporation step from the CA–acetone–methanol casting system. Optimum membranes consist of an ultrathin skin layer, a thin transition layer, and an open-cell, honeycomb-like substructure, and exhibit high selectivities combined with high gas fluxes for the separation of CO_2/CH_4 without the necessity of an additional heat treating and multistage exchange process. It not only depends on the choice of the quench medium, methanol, but is much more relative to the evaporation time during the evaporation process.[4, 5, 18]

To elucidate the importance of the evaporation step for the defect-free integrally skinned asymmetric CA membranes, we analyzed quantitatively the component concentration change during the evaporation process. The behavior of the CA concentration profile in the casting solution for various evaporation times is shown in Figure 2. With increasing evaporation time, CA concentrations in the casting membrane increase, and the CA concentration gradient near the interface is steeper. The concentration distribution of every component in the casting membrane change with the addition of methanol in the casting solution. The saturated vapor pressure of methanol is less than that of acetone. The lower the CA concentration at the interface, the higher the methanol content in the casting membrane because the total evaporation rate decrease under the same evaporation time. But the concentrations of the components versus the substrate side of the casting membrane remain nearly unchanged.

Although the evaporation process is absolutely necessary for the preparation of the defect-free integrally skinned asymmetric CA membranes, the quench step of membrane formation, at which time solvent–nonsolvent exchange and eventual polymer precipitation take place, plays a controlling role in the determination of ultimate membrane structure. Hence, only under the appropriate combination of evaporation conditions and quench steps can the ideal morphological structure with defect-free, ultrathin skin, loose support layer be obtained. A ternary thermodynamic diagram of the methanol–acetone–CA system is shown in Figure 3.[18] Curves A and B represent the concentration profiles in the casting membrane at the end of the evaporation step and prior to quenching, respectively. Curves C and D represent typical quenching composition paths in the membrane at the point of phase separation at low and high CA concentration in the casting membrane, respectively, which were estimated by Tsay's ternary quench process.[13]

Computational results and experiments have shown that without evaporation and even if there is no methanol in the casting solution, the whole of the casting membranes between the CA concentrations of 17 ~25 wt % by the wet phase inversion induce spinodal decomposition (as shown in Figure 4 of reference 4 and in Figure 5-3 in reference 5). Furthermore, experimental separation performances of the membrane for the mixture of CO_2/CH_4 are low. The computational predictions are in agreement with experimental measurement and morphological structure. But when there exists an evaporation step prior to the wet inversion, the initial composition location of the casting

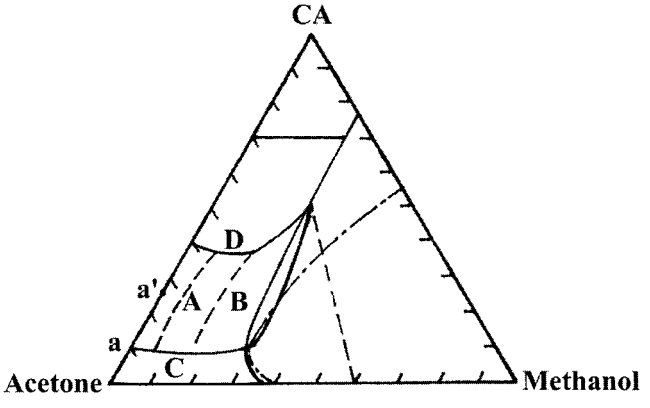

Figure 3 The ternary phase diagram for methanol–acetone–CA system and casting membrane profiles associated with evaporation and quench steps.[13, 18] The composition path for casting solution of 17 wt % CA concentration at the end of evaporation period: line aa': 0 wt % methanol; line A: 5 wt % methanol; line B: 15 wt % methanol; line C: spinodal decomposition concentration profile from substructure; line D: the concentration profile of the skin layer with higher CA concentration.

membrane on the ternary diagram will change significantly, as shown in line aa', path A, path B at the beginning of the quench step. The higher the methanol in the casting membrane, the closer to the binodal curves the initial concentration profile location on the ternary phase diagram. However, even in the presence of an evaporation step, the gas separation performance of the membrane prepared by the binary casting solution of acetone–CA without methanol is still unsatisfactory (as shown in reference 5). In the presence of an evaporation step, the initial concentration profile of the casting membrane will be nonuniform, as shown in line aa' of Figure 3. When the membranes were immersed in the coagulation of methanol, there was a certain time interval between the moment of immersion of the casting solution in the bath of methanol and the onset of demixing. During this so-called delay time, there is a large outflow of acetone from the casting nonuniform membrane, whereas the inflow of methanol is relatively small. In particular, the CA concentration of skin layer in the casting membrane prior to quench is higher. Therefore, the CA concentration will increase further; that is, line aa' will extend up along the axis of CA–acetone. The diffusion rate of methanol in the skin layer will reduce. And, because there is no methanol at the initial casting membrane, it will take a longer time to induce the spinodal decomposition of the substructure by the diffusion of enough methanol into it. During this period, not only the skin layer becomes thicker and denser, but the denser transition layer will appear. The thicker, denser transition layer will make the substructure resistant to a gas transport increase, so that the membrane performance for the separation of CO_2/CH_4 decreases.

With the increase of methanol in the cast solution, the ratio of methanol in the casting membrane will increase because more acetone evaporates and diffuses into the coagulation bath of methanol in the delayed interval. So, the composition change of the skin layer could be reasonably hypothesized as path D. Although the CA concentration of the skin layer is higher, sufficient methanol in the substructure that maintained a low CA initial concentration still provided with the possibility of spinodal decomposition. In addition, the ultrathinness of the skin layer with high CA concentration is also an essential requirement to induce the spinodal decomposition because the medium methanol in the coagulation bath diffuses rapidly across the thinner skin layer and spreads into the substructure.[5] Although the substructure at the much higher methanol content over a value in the casting solution induces spinodal decomposition in the quench, the methanol ratio of the skin layer increases possibly across the binodal line and makes a microphase separation by the nucleation and growth mechanism even during the evaporation step because the volatility of acetone is greater than that of methanol. Obviously, such skin layers contained defects or pores. Hence, in the presence of an evaporation step, the substructure of the casting membrane made from methanol–acetone–CA system still remains the characteristic on the fast spinodal decomposition only when methanol content in the casting solution is in the range 5–15 wt %.

Evaporation steps prior to the quench process have played a decisive role in the formation of the defect-free, ultrathin skin at the top of the open-cell substructure for methanol–acetone–CA system. In Cahn's pioneering work on spinodal decomposition, it was pointed out that a finely mazed three-dimensional network evolves during the initial stages of spinodal decomposition.[31, 32] However, coarsening of the original network occurs at later stages of the phase separation process as a result of the interfacial tension between the two phases. This process leads eventually to a partial decomposed liquid–liquid phase separated morphology consisting of a highly regular, bicontinous network of the polymer-rich and the polymer-poor phases. The spinodal structure, which is microporous, only meets one of the three requirements for ideal asymmetrical membrane for gas separations; that is, the substructure should not contribute any resistance to gas transport, but provide sufficient mechanical strength to support the delicate skin layer during high pressure operation.[34] If the defect-free, ultrathin-skinned layer would form on the spinodal substructure simultaneously, then the skin layer must be provided with at least the following conditions: (1) the skin layer itself has an ability to suppress liquid–liquid phase separation by nucleation and growth or by spinodal decomposition; and (2) the tensile strength of skin layer is high enough to avoid the rupture that would be caused by the spinodal phase separation from the substructure. Wijmans et al. have testified that at high polymer concentrations, polymer solutions are able to form a three-dimensional network and, in that case, the fluid system is transformed into a gel.[35] The gelation has an ability to suppress liquid–liquid phase separation.

The modulus versus temperature for amorphous polymers typically has five regions of behavior, as shown schematically in Figure 4.[33] By analogy, at a constant temperature, the modulus of the phase-separated polymer-rich phase is a strong function of the amount of solvent present and can change due to evaporation. Loss of plasticizing solvent from the polymer-rich phase in this case is analogous to reducing the temperature in the aforementioned plot for pure polymer. In the isothermal solvent-moderated case, if the effective glass transition temperature of the polymer-rich phase approaches the casting temperature, its modulus quickly rises by orders of magnitude and loses deformability. Burghardt et al. also have shown that a glass transition line exists on the ternary diagram.[36] Although CA concentration at the interface also increases considerably during the delay time of

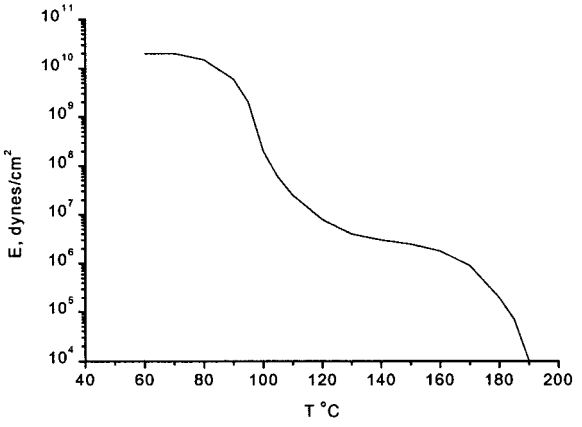

Figure 4 The modulus versus temperature for a typical amorphous polymer.[33]

several minutes that exists prior to the spinodal decomposition even for methanol wet phase inversion without evaporation, the experimental results have shown that the tensile strength of the concentrated CA skin layer increased during this delayed interval is not high enough to resist the interfacial tension caused by the spinodal decomposition of the substructure. Therefore, the addition of the evaporation step and the following quench must make the CA concentration of the skin layer increase and the tensile strength greater than the interfacial tension from the spinodal decomposition. It is shown that the evaporation time >20–40 s can meet the requirement. We will report the dynamic analysis during the quench in a future publication.

CONCLUSIONS

A ternary diffusion model was developed for the evaporation step of the phase inversion process. Calculations were carried out for the methanol–acetone–CA ternary casting system to illustrate the importance of the evaporation step for the defect-free, ultrathin skinned asymmetric CA membrane for the separation of CO_2/CH_4. The combined analysis of quantitatively computational results from the ternary evaporation model and qualitative dynamic results during the quench process have shown that the skin layer of high CA concentration obtained by evaporation has an ability to suppress liquid–liquid phase separation. Furthermore, the skin layer with high tensile strength can resist the interfacial tension caused by spinodal decomposition from the substructure.

Although the CA concentration in the skin layer increased considerably because of the evaporation step and the following delay time during the quench process, the substructure can still induce the spinodal decomposition because the strong coagulant, methanol, can diffuse rapidly across the ultrathin skin layer containing a high content of methanol. Hence, the defect-free, ultrathin-skinned asymmetric membrane for gas separation can be prepared from the methanol–acetone–CA casting system by an evaporation step and the wet phase inversion.

The work described in this paper was financially supported by the Ph.D. Research Foundation of Education Ministry of China.

References

1. Van't Hof, J. A.; Reuvers, A. J.; Boom, R. M.; Rolevink, H. H. M.; Smolders, C. A. J Membr Sci 1992, 70, 17.
2. Pinnau, I.; Koros, W. J. U.S. Pat. 4,902,422 (1992).
3. Pinnau, I.; Koros, W. J. J Membr Sci 1992, 71, 81.
4. Hao, J. H.; Wang, S. C. J Appl Polym Sci 1998, 68, 1269.
5. Hao, J. H.; Wang, S. C. Ph.D. Dissertation, Tianjin University, Tianjin, P. R. China, 1995.
6. Anderson, J. E.; Ullman, R. J Appl Phys 1973, 44, 4303.
7. Ataka, M.; Sasaki, K. J Membr Sci 1982, 11, 11.
8. Castellari, C.; Ottani, S. J Membr Sci 1981, 3, 29.
9. Castellari, C,; Ottani, S. Desalination 1988, 69, 223.
10. Krantz, W. B.; Ray, R. J.; Sani, R. L.; Gleason, K. J. J Membr Sci 1986, 29, 11.
11. Tsay, C. S.; McHugh, A. J. J Membr Sci 1991, 64, 81.
12. Wang, Z. Ph.D. Dissertation, Tianjin University, Tianjin, P. R. China, 1993.
13. Tsay, C. S.; McHugh, A. J. J Polym Sci, Part B: Polym Phys 1990, 28, 1327.
14. Tsay, C. S.; McHugh, A. J. Chem Eng Sci 1991, 46, 1179.
15. Bird, R. B.; Stewart, W. E.; Lightfoot, E. N. Transport Phenomena; Wiley: New York, 1982.
16. Yilmaz, L.; McHugh, A. J. J Membr Sci 1986, 28, 287.
17. Smith, J. M.; Van Ness, H. C. Introduction to Chemical Engineering Thermodynamics; McGraw-Hill: New York, 1987.
18. Hao, J. H.; Wang, S. C. J Appl Polym Sci 2001, 80, 1650.
19. McAdams, W. H. Heat Transmission, 3rd ed.; McGraw-Hill: New York, 1954.
20. Vrentas, J. S.; Duda, J. L.; Ling, H. C. J Appl Polym Sci 1986, 31, 997.
21. Reuvers, A. J.; van den Berg, J. W. A.; Smolders, C. A. J Membr Sci 1987, 34, 45.
22. Bearman, R. J. J Phys Chem 1961, 65, 1961.
23. Reid, R. C.; Prausmitz, J. M.; Poling, S. E. The Properties of Gases and Liquids; McGraw Hill Book Company: New York, 1987.
24. Laatikainen, M.; Lindstrom, M. Acta Polytech Scand, Chem Technol Metall Ser 1986, 175, 61.
25. Bennett, C. O.; Myers, J. E. Momentum, Heat, and Mass Transfer, 3rd ed.; McGraw-Hill: New York, 1982
26. Yin, Y. J. University Chemistry Handbook; Shandong Sinence & Technology Press: Jinan, 1985
27. Perry, R. H. Perry's Chemical Engineerings' Handbook, 6th ed.;
28. Brokaw, R. S. Ind Eng Chem Proc Des Dev 1969, 8, 240.
29. Lu, H. Z. Handbook on Petrochemical Basic Data; Chemical Industry Press: Beijing, 1980.
30. Tianjin University. Transport Process of Chemical Process; Chemical Industry Press; Beijing, 1980.
31. Cahn, J. W. J Chem Phys 1965, 42, 93.
32. Cahn, J. W.; Charles, R. J. Phys Chem Glasses 1965, 6, 181.
33. Aklonis, J. J.; MacKnight, W. J. Introduction to Polymer Viscoelasticity, 2nd ed.; Wiley-Interscience Publisher, John Wiley and Sons: New York, 1983; pp. 40–45.
34. Pinnau, I.; Koros, W. J. J Polym Sci, Part B: Polym Phys 1993, 31, 419.
35. Wijmans, J. G.; Kant, J.; Mulder, M. H. V.; Smolders, C.A. Polymer 1985, 26, 1539.
36. Burghardt, W. R.; Yilmaz, L.; McHugh, A. J. Polymer 1987, 28, 2085.